



Climate Change in Jordan: A Case Study of Yarmouk Basin Using Statistical Downscaling Model

Abdelaziz Q. Bashabsheh^{1)*}, *Kamel K. Alzboon*²⁾

¹⁾ Engineer, Environmental Engineering Department, Al-Huson University College, Al-Balqa' Applied University, Irbid, Jordan.

* Corresponding Author. E-Mail: Abdelazizbashabsheh@gmail.com

²⁾ Prof., Environmental Engineering Department, Al-Huson University College, Al-Balqa Applied University, Irbid, Jordan. E-Mail: alzboon@bau.edu.jo

ARTICLE INFO

Article History:

Received: 2/1/2025

Accepted: 17/5/2025

ABSTRACT

This study evaluates the impacts of climate change in the Yarmouk River Basin (YRB) using the Statistical Downscaling Model (SDSM) and observed data from six meteorological stations (1989-2017). The second-generation Canadian Earth System Model (CanESM2) was used to project climate scenarios under Representative Concentration Pathways (RCPs) for the period 2018-2100, demonstrating strong performance in modeling the arid climate ($R^2 = 0.87-0.996$, RMSE = 0.478-1.829 for calibration; $R^2 = 0.799-0.998$, RMSE = 0.55-1.879 for validation). Projected maximum temperature increases across the basin range from 0.19 °C to 1.8 °C, while minimum temperature rises from 0.096 °C to 1.4 °C, depending on emission scenarios. Precipitation is expected to decline by 3% to 49%, with the most severe reductions under RCP8.5. Moreover, current climate observations indicate sharper temperature increases and precipitation declines than even RCP8.5 projections, signaling elevated risks of drought and water scarcity.

The analysis of extreme events reveals substantial increases in heatwaves, notable declines in cold spells, and longer dry periods across all scenarios. Under RCP8.5, heatwave days may rise by up to 22, cold spells may drop by more than 24 days, and consecutive dry days could extend by over 65 days, suggesting intensified drought stress.

A frequency analysis of the 12-month Standardized Precipitation Index (SPI-12) reveals relatively stable hydro-climatic conditions under RCP2.6, with a balanced distribution of dry and wet months and minimal extremes. Under RCP4.5, a modest shift toward drier conditions emerges, with slightly increased drought frequencies and minor extreme events. In contrast, RCP8.5 projects pronounced drying, with over 40% of months falling below SPI = -0.5 in Irbid and Al-Mafraq, and rising frequencies of both extreme drought and wet months in Samar. These progressive changes highlight the basin's vulnerability to emission-driven climate impacts and underscore the urgent need for adaptation planning. The findings support the SDSM-CanESM2 framework as a robust tool for assessing climate risks and guiding mitigation strategies in arid and semi-arid regions.

Keywords: Climate change, Yarmouk River Basin, Statistical Downscaling Model (SDSM), CanESM2, Representative Concentration Pathways (RCPs), Extreme climate events, Drought, Standardized Precipitation Index (SPI-12), Hydro-climatic variability, Arid and semi-arid regions, Future climate projections.

INTRODUCTION

Climate change can be defined as a natural process of long-term changes in climatic elements and weather patterns (United Nations, 2022). Recently, a fast rise in temperatures resulting from human activities was noticed mainly due to the burning of fossil fuels which generate greenhouse gas emissions (IPCC, 2022). There is no doubt that human practices have led to an increase in the temperatures of the atmosphere, oceans, and land. A rapid and widespread change has been observed in the atmosphere, oceans, cryosphere, and biosphere. Greenhouse gas (GHG) concentrations are now at their peak for at least the past 2 million years and the emissions keep increasing. As a result, the earth's temperature increased by approximately 1.1°C compared to its temperature before the industrial revolution (WMO, 2022; IPCC, 2021). The last decade was the warmest on record, which led to a large-scale damage associated with losses and damages to nature and people, beyond natural climate variability (Langsdorf et al., 2022).

The Middle East and the neighboring Mediterranean countries are known for their high vulnerability to climate change due to their arid and semi-arid climate, water scarcity, high birth rates, difficult political and economic conditions, and large numbers of displaced people (Linares et al., 2020; Al Qatarnah et al., 2022; Giorgi et al., 2008).

Jordan has experienced an increase in climate-related hazards in recent years, including extreme temperatures, droughts, floods, and landslides. These hazards have become more frequent and intense due to human-induced climate change. Floods, in particular, have caused a significant damage, resulting in loss of lives, destruction of agricultural lands, infrastructure damage, and landslides (NCCAPJ, 2021; Alzboon et al., 2021). Over the past six decades, annual maximum temperatures in Jordan have risen by 0.3°C to 1.8°C, while annual minimum temperatures have increased by 0.4°C to 2.8°C. The frequency of heatwaves and consecutive dry days has grown, while annual rainfall has decreased by 5%-20% (USAID, 2017). Furthermore, 92% of total precipitation is lost to evaporation (Barjenbruch et al., 2010). Al Qatarnah et al. (2022) reported an increase in the frequency of hot days ($T_{max} > 38^{\circ}\text{C}$) in the Azraq Basin over the past 46 years, with no significant change in precipitation. They

also projected a rise in evaporation rates by 4.74%-5.32% for Al Butum and El Janab wadis during 2013-2030. Bashabsheh et al. (2024) analyzed data from the Yarmouk River Basin spanning from 1989 to 2017. Their findings revealed that mean maximum and minimum temperatures increased across all stations, with average rises of 1.62°C and 1.39°C, respectively, accompanied by an insignificant change in precipitation trends.

Internationally, a study in the United States that used SDSM to analyze changes in snow cover in the 21st century over the northeastern United States showed that the snow cover will decline sharply by the end of the century (Tryhorn et al., 2012). In the Loess Plateau in China, the SDSM showed an expected increase in the temperature over the entire plateau based on the historical period 1961-1990 (Fan et al., 2021).

The Statistical Downscaling Model (SDSM) was used in previous studies to predict the climate in the Middle East until the end of the current century. Hassan (2020) used the third version of Hadley Centre Coupled Model (HadCM3) to generate climate change scenarios for the Iraqi western desert. The results predicted an increase in annual precipitation and in average temperature for scenarios A2 and B2. El Raey et al. (2016) used HadCM3 and selected the A2 and B2 scenarios to downscale climate change in Alexandria city and the results showed an increase in the mean temperature and a decrease in precipitation.

In Jordan, Raggad et al. (2016) used the statistical downscaling method to assess the effect of climate change on groundwater resources in Ajlun by using different GCMs, and the results showed that the maximum temperature will increase by 1.7 °C, the minimum temperature will increase by 2.2 °C, and the rainfall will decrease by 18.7% by the mid of the 21st century. Abdulla (2020) used HadCM3 to generate scenarios for the base period (1961-2014), and the results showed an increase in temperature between (2.5 C –5 °C), and a decrease in precipitation by a value ranging from (10%-37%). According to projections under the RCP scenarios, mean maximum temperatures are expected to rise by 0.32°C to 1.52°C, while precipitation levels are projected to decrease between 8.5% and 43.0% throughout the 21st century (Bashabsheh et al., 2024).

This research will concentrate on the Yarmouk River Basin area due to its vital importance to Jordan's

agricultural sector. The Yarmouk River generally provides 40% of Jordan's surface water and is considered as the main source for the King Abdullah Canal, which is essential for the development of the Jordan Valley (FAO, 2023). Numerous studies have examined the impacts of climate change in the region. However, these studies primarily focus on general trends and do not fully address how current climatic conditions deviate from projected scenarios or provide predictions of future extreme climate events.

Building on the work of Bashabsheh et al. (2024), who used the Statistical Downscaling Model (SDSM) to evaluate climate change impacts on water resources in the Yarmouk River Basin. This study expands the model's application to include a comprehensive analysis of drought frequency and intensity. By integrating SPI-12 (12-month Standardized Precipitation Index) analysis under three RCP scenarios (2.6, 4.5, and 8.5), the study assesses long-term hydro-climatic variability and the likelihood of extreme dry or wet periods. This approach not only enhances the understanding of future drought risks and predicts potential extreme climate events, but also evaluates the performance and reliability of the CanESM2 model in simulating climate conditions in arid and semi-arid regions. Additionally, the study examines the spatial distribution of projected changes across key sub-regions and compares current climate patterns with future projections, reinforcing the model's potential as a valuable tool for climate adaptation

planning in vulnerable, water-scarce environments.

METHODOLOGY

Study Area and Data

The study area is the Jordanian side of the Yarmouk River Basin (YRB) with an area of 1424 km² in the north of Jordan, as shown in Figure (1). The climate in the YRB is "Mediterranean" sub-tropical; it is characterized as semi-arid with hot and dry summers and cold and wet winters (Kottek et al., 2006). The mean precipitation on the Jordanian side of the basin ranges between 600 mm in the western parts and less than 150 mm in the east. The wet season initiates in November and ends in May (Al-Bakri et al., 2011), and the mean temperatures vary from 30°C to 13°C in the lowlands and from 18°C to 10°C in the highlands. The highest point of the basin in Jordan is located in Ajloun Governorate with an elevation of more than 1200 m ASL (above sea level) and the lowest point lies at the confluence with the Jordan River, which is the basin outlet with an elevation of about 247 m BSL.

Three meteorological stations, and three precipitation stations with data ranging from 1989 to 2017 were used to study the consequences of the main climate change indicators (temperature, and rainfall). The daily data covers the records of 3 variables: minimum temperature, maximum temperature, and precipitation.

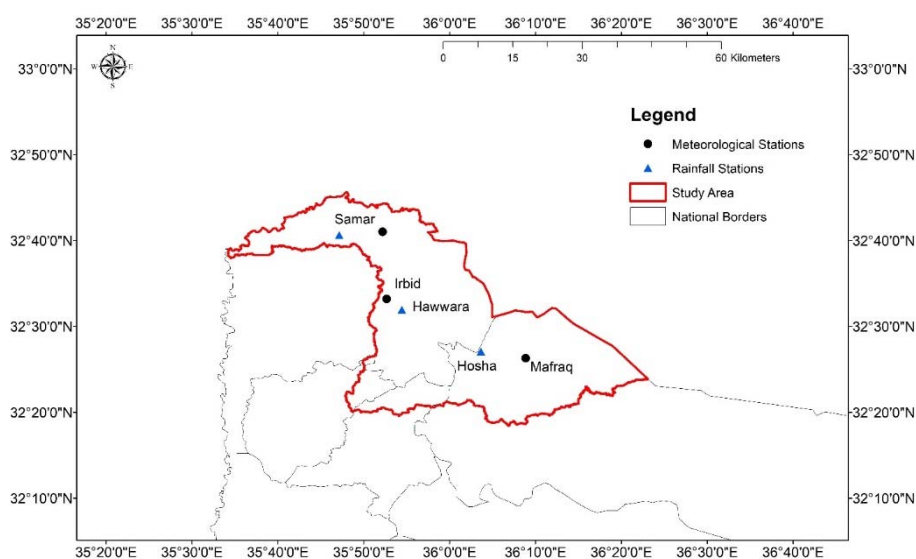


Figure (1): The study area with the meteorological stations

STATISTICAL DOWNSCALING MODEL

Downscaling translates coarse Global Climate Model (GCM) output into finer, local-scale projections that are suitable for hydrological and impact studies (Fowler et al., 2007). Two principal approaches exist: dynamical downscaling, which embeds a high-resolution Regional Climate Model within GCM fields, and statistical downscaling, which derives empirical relationships between large-scale predictors and local climate (Fowler et al., 2007). Among statistical methods, the Statistical Downscaling Model (SDSM) is widely used for quantifying mean and extreme climate change impacts (Wilby et al., 2002; Dibike et al., 2008; Hashmi et al., 2011). SDSM combines multiple linear regression with a stochastic weather generator to reproduce daily station-scale temperature and precipitation, offering simplicity, computational efficiency, and robust performance where calibration statistics are strong (R^2 typically >0.8). Its primary limitation lies in the assumption of stationarity—that predictor–predictand relationships remain constant under future climates—which cannot be directly tested (Fowler et al., 2007). Despite this, SDSM has been recommended by the Canadian Climate Impact Scenarios Project (CCIS) and successfully applied in numerous semi-arid and arid basins, making it an appropriate choice for the Yarmouk River Basin study (Wilby et al., 2004). The Canadian Earth System Model version 2 (CanESM2) has demonstrated strong applicability for climate projections in arid and semi-arid regions, such as the Yarmouk River Basin, due to its consistent performance and computational efficiency. In the Yarmouk Basin, CanESM2 projected temperature increases ranging from 0.9°C to 3.2°C and precipitation decreases between 9.5% and 31.6% across RCP scenarios for the period 2011–2099, aligning with observed regional drying trends (Abdulla et al. 2021).

Compared to more computationally intensive models like GFDL-ESM2M and HadGEM2-ES, CanESM2 maintains accuracy while requiring less processing time for century-scale simulations. As a core contributor to the Coupled Model Intercomparison

Project Phase 5 (CMIP5), CanESM2 ensures standardized outputs that are directly comparable with over 40 other GCMs. In the northwest region of Bangladesh, studies have shown that after bias correction, the CanESM2-based downscaling model performs better compared to the HadCM3-based model, making it a preferred choice for regional climate assessments (Kumar et al., 2013; Rana et al., 2024).

While CanESM2 has documented biases, its integration with quantile mapping and SDSM—demonstrated in northwest Bangladesh with a 12.5% RMSE reduction (Rana et al., 2024), and validated in the ClimEx project for improved extreme precipitation modeling (Leduc et al., 2019)—makes it a robust choice for Mediterranean basins like the Yarmouk Basin. Its balance of accuracy, computational efficiency, and compatibility with statistical downscaling protocols justifies its use despite inherent limitations, which are systematically addressed.

Statistical downscaling method was used to downscale the climatic variable utilizing the second generation of the Earth System Model (CanESM2). SDSM software was downloaded from <https://sdsml.org.uk/software.html>. Predictand parameters in this study are the precipitation and maximum and minimum temperatures. The software applies sundry tasks: quality control, data transformation; predictor variable screening; model calibration; weather generation; statistical analyses, and scenario generation. Screening predictors are the major step to obtaining a more certain downscaling process (Wilby et al., 2002; Huang et al., 2011). Figure (2) illustrates the structure of SDSM [Wilby et al., 2007].

Selection of Predictors

The National Centre for Environmental Prediction (NCEP) suggested 26 predictor variables (Table 1) for producing ensembles of synthetic daily weather series. The predictors are created by state-of-the-art assimilation of all available observed climate data into a global climate-forecasting model that produces interpolated grid results of many climate variables (Saha et al., 2010; Wilby et al., 2007).

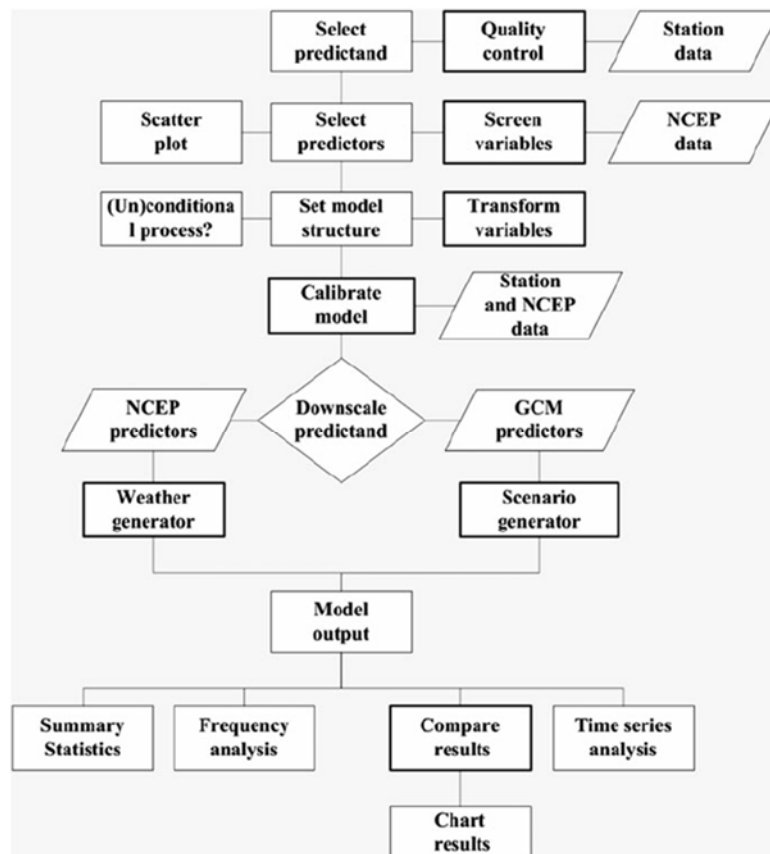


Figure (2): Structure of SDSM

Table 1. NCEP predictor variables available in SDSM

Number	Predictor	Description	Number	Predictor	Description
		Code			Code
1	p_f	Surface airflow strength	14	r500	500 hPa relative humidity
2	p_u	Surface zonal velocity	15	p8_f	850 hPa airflow strength
3	p_v	Surface meridional velocity	16	p8_u	850 hPa zonal velocity
4	p_z	Surface vorticity	17	p8_v	850 hPa meridional velocity
5	p_th	Surface wind direction	18	p8_z	850 hPa vorticity
6	p_zh	Surface divergence	19	p8th	850 hPa wind direction
7	rhum	Surface relative humidity	20	p8zh	850 hPa divergence
8	p5_f	500 hPa airflow strength	21	r850	850 hPa relative humidity
9	p5_u	500 hPa zonal velocity	22	p500	500 hPa geopotential height
10	p5_v	500 hPa meridional velocity	23	p850	850 hPa geopotential height
11	p5_z	500 hPa vorticity	24	Temp	Mean temperature at 2m
12	p5th	500 hPa wind direction	25	Shum	Surface-specific humidity
13	p5zh	500 hPa divergence	26	Mslp	Mean sea level pressure

This process is performed by constructing multi-linear regression equations *via* dual simplex or ordinary least square algorithms between predict and the NCEP predictors that are determined through the screening of variables step. Screening variables is the most important

step of the statistical downscaling method to select relevant downscaling predictor variables, which highly impact the generated scenarios (Wilby et al., 2007). SDSM creates a correlation matrix and shows the correlation variances between the predictand and 26

NCEP predictors. Predictors with a high correlation to the predictand (p -value <0.05) were selected for the weather and scenario generator.

Model Calibration and Validation

SDSM software provides two process methods to model calibration depending on climate data. The first process is called the conditional process, which suggests that there is an indirect link between the climate data and predictors; this process is used for precipitation data and is dependent on the regional scale predictors. The second process is called the unconditional process, which supposes that there is a direct link between the climate data and predictors. This process is used for temperature data (Wilby et al., 2007).

The historical data is split into two periods: the first period is for calibration (1989–2000), and the second period is for validation (2001–2017). These performance indices are applied to assess the performance of the model: coefficient of determination (R^2), and as well as Root Mean Square Error (RMSE).

Scenarios Generation

The second generation of the Earth System Model (CanESM2) is a user model to assess the changes in future climate. This model produces climate change scenarios using GHG Representative Concentration Pathways (RCPs). RCPs reflect the greenhouse gas concentration of several possible future climate pathways for human greenhouse gas emissions expressing a rise in the potential radiative forcing values compared to pre-industrial values by 2100. Three RCPs were used in this research (Clarke et al., 2014):

1. RCP 2.6, strict mitigation scenario. Radiation is equal to 2.6 W/m^2 .
2. RCP 4.5, moderate scenario. Radiation is equal to 4.5 W/m^2 .
3. RCP 8.5, very high GHG emissions. Radiation is equal to 8.5 W/m^2 .

Extreme Climate Events Projection

In this research, three indices were identified and analyzed as indicators of extreme climate events; namely:

1. Heatwaves: The proportion of days when the maximum temperature exceeds the 90th percentile.
2. Cold Spells: The proportion of days when the minimum temperature falls below the 10th percentile.

3. Consecutive Dry Days: The longest sequence of consecutive days with precipitation less than 1 mm.

These indices were computed using Excel, leveraging data analysis functions to process the climate data and calculate the thresholds for each event.

Standardized Precipitation Index (SPI) Calculation

The Standardized Precipitation Index (SPI) was applied to assess drought and wetness conditions at a 12-month timescale (SPI-12) for the Yarmouk River Basin (YRB). Monthly precipitation data for the period (2020–2100) under different climate scenarios (RCP2.6, RCP4.5, and RCP8.5) were used as input. The calculation process followed the World Meteorological Organization (WMO) recommended procedures to ensure standardized and comparable results.

SPI values were calculated using the SPI Calculator (WMO Recommended) and the SPI Generator software developed by the National Drought Mitigation Center (NDMC) (WMO, 2012; NDMC, 2018). The SPI values interpret climatic conditions as follows:

Table 2. SPI value interpretation scale

SPI Value Range	Interpretation
$\text{SPI} \geq 2.0$	Extremely wet
$1.5 \leq \text{SPI} < 2.0$	Very wet
$1.0 \leq \text{SPI} < 1.5$	Moderately wet
$-1.0 < \text{SPI} < 1.0$	Near normal
$-1.5 < \text{SPI} \leq -1.0$	Moderately dry
$-2.0 < \text{SPI} \leq -1.5$	Severely dry
$\text{SPI} \leq -2.0$	Extremely dry

RESULTS AND DISCUSSION

Results of Predictor Selection

Thirteen predictors exhibited high correlations, while the remaining predictors showed low correlations, as outlined in the analysis. Temperature predictors generally displayed a stronger correlation compared to precipitation predictors.

For Irbid station (Temperature), several predictors were highly correlated, including p1_zh, p5_z, and p500. Shum and Temp also showed significant correlations with temperature at this station. On the other hand, Mslp and p850 showed weaker correlations.

For Al-Mafraq station (Temperature), p1_zh, p5_z, p500, Shum, and Temp were strongly correlated with

temperature. In contrast, p1_u and p8_u showed only weak correlations.

At Samar station (Temperature), p1_zh, p5_z, p500, Shum, and Temp were also highly correlated with temperature. Other predictors, such as p8_v and p5_u, showed weaker correlations.

For precipitation predictors, both Irbid and Al-Mafraq stations demonstrated a few high correlations, particularly with p1_zh, Temp, and p850, while other precipitation-related predictors, such as p8_u, s_500, and p5_f, were less correlated. The Samar station (Precipitation) showed a similar pattern, with Temp and p8_v being the most significant predictors for precipitation.

Model Calibration and Validation

To effectively run the SDSM model, a calibration process was carried out to establish the relationship between predictands (observed temperature and precipitation) and large-scale predictors. This step was essential was applying the model to future climate projections using GCM outputs. Observed maximum temperature (Tmax), minimum temperature (Tmin), and precipitation (Prcp) data was used for both calibration and validation phases. As summarized in Table 3, the coefficient of determination (R²) values for daily simulated and observed temperatures were remarkably high across all stations, consistently exceeding 0.99 during both calibration and validation periods,

indicating a very strong correlation. RMSE values for temperature were also low, ranging from 0.836 to 1.641 suggesting minimal error in simulation.

For precipitation, the model also showed satisfactory performance with R² values during the calibration and validation periods ranging from 0.799 at Al-Mafraq to 0.94 at Samar. Although slightly lower than temperature results, these values still reflect a strong agreement between simulated and observed data. RMSE values for precipitation varied from 0.55 to 1.879 across the stations, which is acceptable given the typically higher variability in precipitation patterns compared to temperature. This comparatively lower accuracy is likely due to the inherent complexity of precipitation modeling, as generating an ideal multiple regression equation for precipitation is challenging due to its conditional nature (Wilby et al., 2004). This limitation has been extensively discussed in prior studies (Wilby et al., 2004; Dibike et al., 2008).

Overall, the statistical metrics summarized in Table 3 suggest that the SDSM model effectively captures the daily variability of both temperature and precipitation. Among the stations, Irbid and Samar stations showed particularly high performance for temperature modeling, while Samar station exhibited the best precipitation simulation. These results confirm the model’s robustness and reliability in downscaling climate variables in the study area.

Table 3. Performance indicators of SDSM during the calibration and validation periods

Station	Calibration Validation			
	R ²	RMSE	R ²	RMSE
Irbid station (Tmax*)	0.9919	1.641	0.998	1.463
Al-Mafraq station (Tmax)	0.994	1.628	0.996	1.512
Samar station (Tmax)	0.996	1.463	0.998	1.235
Irbid station (Tmin*)	0.9956	1.118	0.997	0.915
Al-Mafraq station (Tmin)	0.996	1.165	0.996	1.051
Samar station (Tmin)	0.995	1.054	0.998	0.836
Irbid station (prcp*)	0.92	1.301	0.847	1.689
Samar station(prcp)	0.94	1.829	0.857	1.879
Al-Mafraq station(prcp)	0.87	0.478	0.799	0.550
Tmax= Maximum temperature, Tmin= Minimum temperature, Prcp= precipitation.				

Both the calibration and validation stages were evaluated using monthly bar charts (Figures 3 and 4), which compare observed and modeled values from January to December. These charts offer a more detailed view of the model’s performance across individual months, revealing seasonal patterns and variability that may not be evident in annual time series plots.

Presenting the data on a monthly scale allows for the identification of seasonal biases and enhances the assessment of model reliability.

Overall, the results confirm that SDSM is not only accurate, but also highly adaptable to arid regions, offering reliable predictions for future climate assessments.



Figure (3): Observed and modeled mean monthly maximum temperature, minimum temperature, and precipitation during the calibration period (1989–2000) in the Yarmouk River Basin (YRB)



Figure (4): Observed and modeled mean monthly maximum temperature, minimum temperature, and precipitation during the validation period (2001–2005) in the Yarmouk River Basin (YRB)

Future Climate Projection

Projection of Temperature Trend

The results from the CanESM2 GCM predict an increase in maximum and minimum temperatures and a decrease in precipitation for the three scenarios—RCP2.6, RCP4.5, and RCP8.5—at Irbid, Al-Mafraq, and Samar stations.

Maximum Temperature Trends

- Under RCP2.6, the maximum temperature is projected to increase by 0.024°C/decade in Irbid, 0.058°C/decade in Al-Mafraq, and 0.047°C/decade

in Samar.

- RCP4.5 forecasts higher increases: 0.075°C/decade, 0.105°C/decade, and 0.1°C/decade, respectively.
- RCP8.5 predicts the most significant rise, with 0.213°C/decade in Irbid, 0.226°C/decade in Al-Mafraq, and 0.192°C/decade in Samar.

By the end of the century:

- Irbid’s maximum temperature is expected to increase by 0.192°C, 0.6°C, and 1.7°C for RCP2.6, RCP4.5, and RCP8.5, respectively.
- Al-Mafraq’s maximum temperature is anticipated to rise by 0.464°C, 0.84°C, and 1.8°C, respectively.

- Samar’s maximum temperature is projected to increase by 0.376°C, 0.8°C, and 1.54°C, respectively.

The rates of increase in maximum temperatures are expected to be greater in Al-Mafraq and Samar than in Irbid.

Minimum Temperature Trends

- RCP2.6 projects a rise in minimum temperatures by 0.025°C/decade in Irbid, 0.019°C/decade in Al-Mafraq, and 0.012°C/decade in Samar.
- RCP4.5 predicts increases of 0.067°C/decade, 0.061°C/decade, and 0.053°C/decade, respectively.
- RCP8.5 anticipates the highest rise in minimum temperatures: 0.175°C/decade in Irbid, 0.159°C/decade in Al-Mafraq, and 0.144°C/decade in Samar.

By the end of the century:

- The minimum temperature in Irbid is expected to increase by 0.2°C, 0.536°C, and 1.4°C for RCP2.6, RCP4.5, and RCP8.5, respectively.
- Al-Mafraq’s minimum temperature is projected to rise by 0.152°C, 0.48°C, and 1.27°C, respectively.
- Samar’s minimum temperature is expected to increase by 0.096°C, 0.42°C, and 1.15°C, respectively.

Unlike for maximum temperatures, Irbid exhibits the highest increase in minimum temperatures, followed by Al-Mafraq and then by Samar.

These trends are illustrated in Figures 5 and 6, which show the annual changes in maximum and minimum temperatures under all RCP scenarios at the three stations.

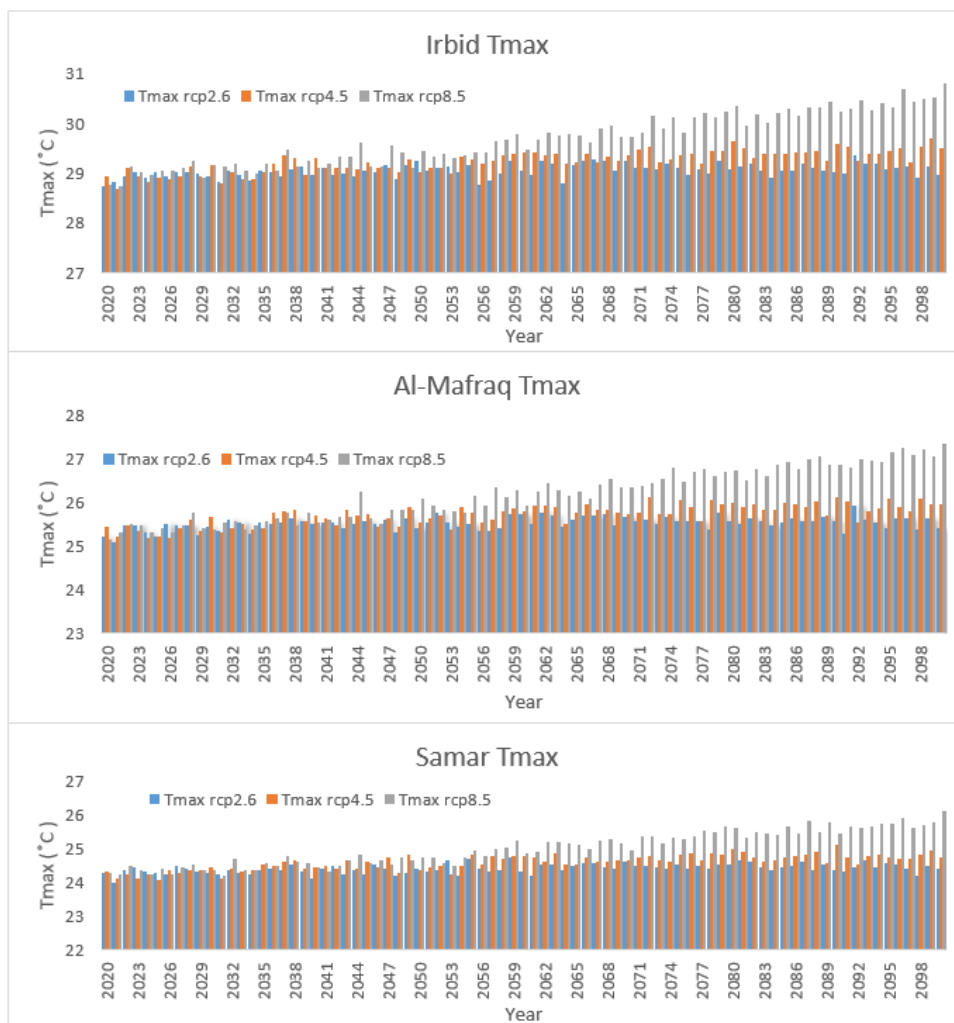


Figure (5): Annual projected maximum temperature trends (2020-2100) under RCP2.6, RCP4.5, and RCP8.5 at Irbid, Al-Mafraq, and Samar stations

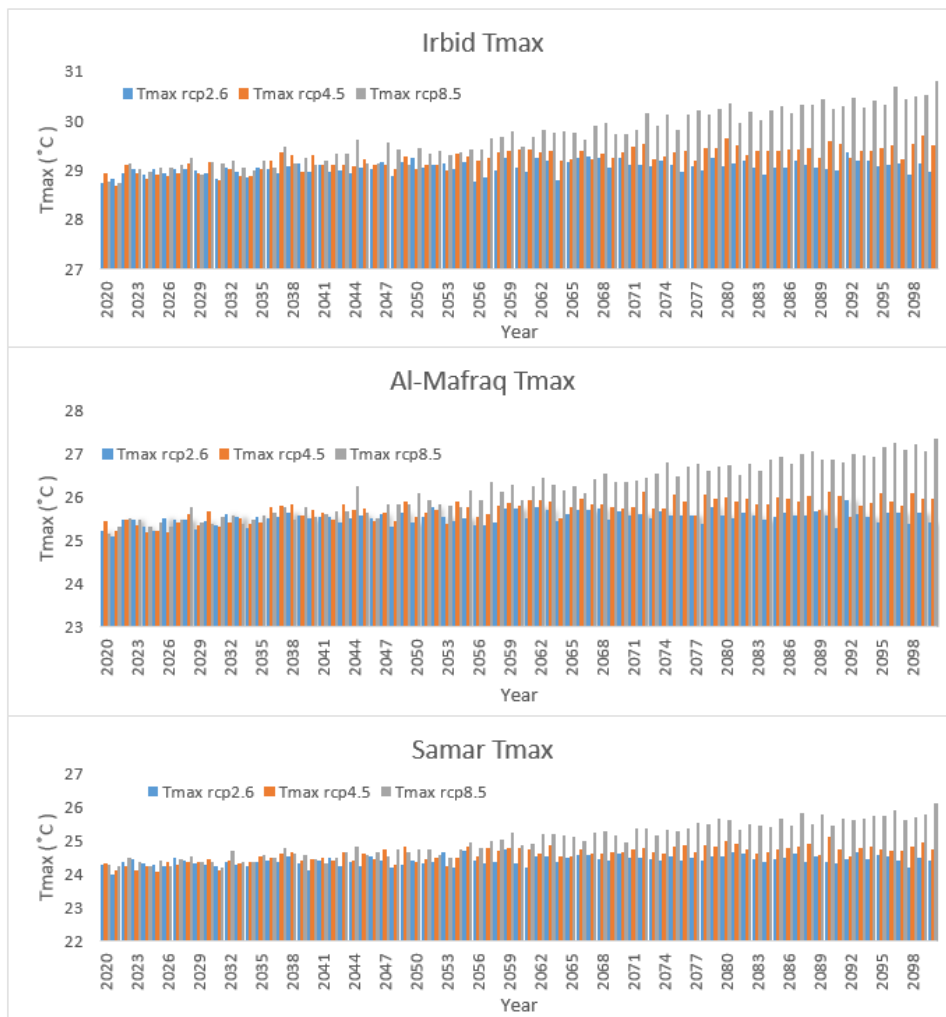


Figure (6): Annual projected minimum temperature trends (2020-2100) under RCP2.6, RCP4.5, and RCP8.5 at Irbid, Al-Mafraq, and Samar stations

Projection of Precipitation Trend

Precipitation is projected to decrease across all three stations:

- **RCP2.6** shows reduction slopes of 0.17, 0.059, and 0.485 in Irbid, Mafraq, and Samar, respectively.
- **RCP4.5** indicates decline slopes of 0.65, 0.25, and 1.12 in the same locations.
- **RCP8.5** predicts significant decrease slopes of 1.93, 0.867, and 2.733, respectively.

By the end of the century:

- Irbid's precipitation is expected to decrease by 3.8%, 14.5%, and 43.2% for RCP2.6, RCP4.5, and RCP8.5, respectively.
- Al-Mafraq's precipitation will decline by 3%, 13%, and 44%, respectively.
- Samar's precipitation is projected to decrease by 9%,

20%, and 49%, respectively.

Samar experiences the highest reduction in precipitation among the three stations, followed by Irbid and then by Al-Mafraq. This aligns with the observation that regions with higher precipitation rates, like Samar, may face more severe impacts from climate change.

These findings align with previous studies, such as Abdulla et al. (2020), which reported 17.6%, 26.1%, and 43.5% reductions in precipitation under RCP2.6, RCP4.5, and RCP8.5 scenarios, respectively, by the end of the century.

Figure 7 presents the annual projected precipitation decline, highlighting the sharper decreases under RCP8.5 compared to RCP2.6 and RCP4.5 at the three stations.

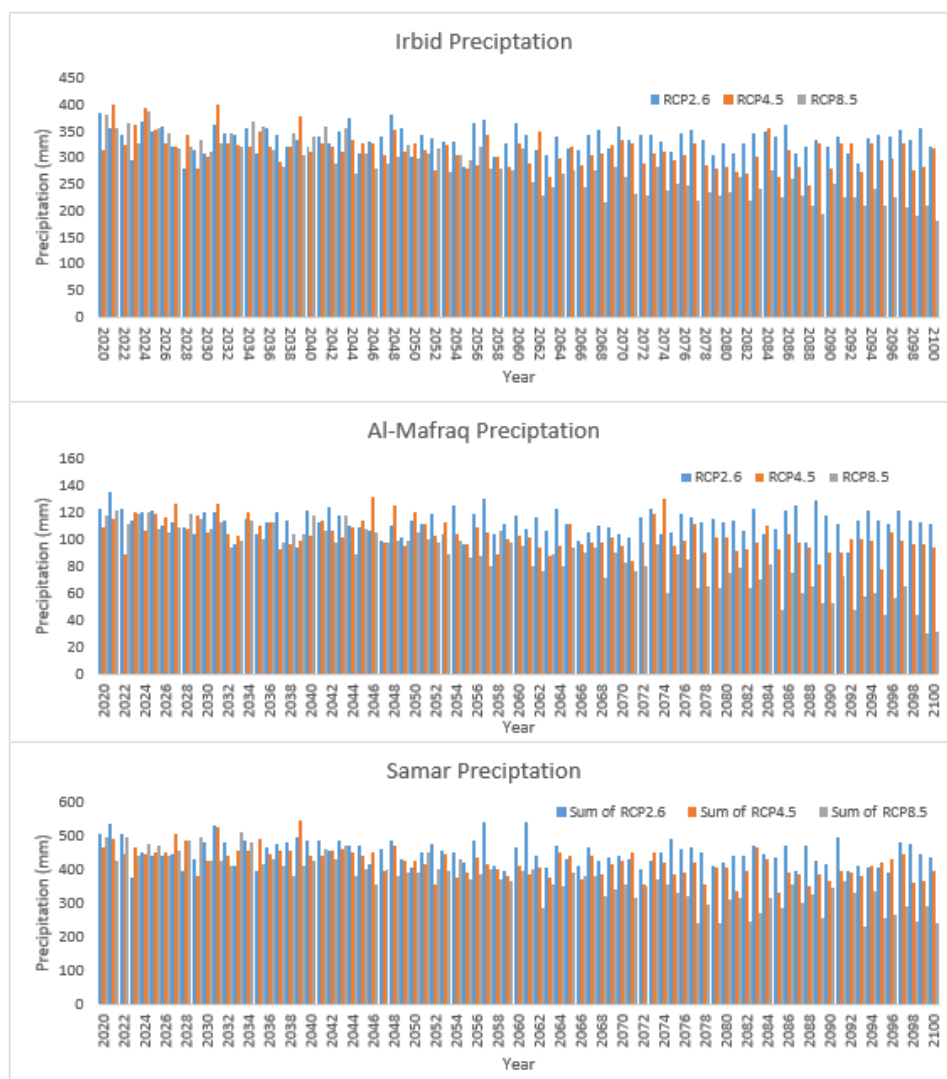


Figure (7): Annual projected precipitation trends (2020–2100) under RCP2.6, RCP4.5, and RCP8.5 at Irbid, Al-Mafraq, and Samar stations

Spatial Distribution of Climate Projections

The spatial distribution analysis of temperature and precipitation trends under the CanESM2 scenarios reveals important regional variations within the basin. This analysis, based on Kriging method (Shtiliyanova et al., 2017), highlights the geographical disparity in climate impacts across the study area.

Temperature Trends

The spatial distribution of temperature changes across the Yarmouk Basin (see Figure (8)) highlights regional variations in projected increases of maximum and minimum temperatures under different RCP scenarios. Although these differences are not dramatic, they provide important insights into localized climate

dynamics. For maximum temperatures, the eastern region characterized by a dry desert climate is projected to experience the highest increases. Under RCP2.6, temperatures in this area are expected to rise by 0.34°C to 0.46°C. This warming intensifies under RCP4.5 and RCP8.5 reaching 0.75°C to 0.84°C and 1.72°C to 1.8°C, respectively. In contrast, the western region, a key agricultural zone, is projected to experience slightly lower increases: 0.19°C to 0.4°C under RCP2.6, 0.6°C to 0.84°C under RCP4.5, and 1.54°C to 1.75°C under RCP8.5.

For minimum temperatures (see Figure (9)), the trend slightly reverses with the western region experiencing higher projected increases. Under RCP2.6, minimum temperatures are expected to rise by 0.096°C

to 0.2°C in the west, and by 0.14°C to 0.16°C in the east. Under RCP4.5, these values increase to 0.42°C to 0.84°C in the west, and to 0.47°C to 0.49°C in the east. RCP8.5 shows the sharpest increases, with 1.0°C to 1.4°C in the west and with 1.26°C to 1.3°C in the east. Despite the relatively small differences, these rising temperatures are concerning, especially in a basin dominated by evaporation processes (Bashabsheh et al., 2024).

Precipitation Trends

The spatial analysis of projected precipitation changes (see Figure (10)) reveals a general decline across the Yarmouk Basin, with the most significant reductions occurring in the western region, which is vital for Jordan’s agricultural productivity. Under RCP2.6, precipitation in the eastern region is expected to decrease by 3% to 3.9%, while the western region may experience more substantial declines ranging from 3.9% to 9%. These reductions become more severe under higher-emission scenarios. Under RCP4.5, precipitation in the western region is projected to decline by 14.2% to 20%, and under RCP8.5 by an alarming 44% to 49%.

Although the eastern region also faces considerable declines ranging from 43% to 45.3% under RCP8.5, the impact is expected to be more pronounced in the west where water scarcity is already a critical issue. This disparity underscores the growing vulnerability of the western basin to drought and highlights the potential for worsening water shortages and agricultural stress.

The implications for agriculture are particularly concerning. The western region, known for producing olives, grains, and honey, is likely to suffer severe setbacks due to the dual threats of increasing temperatures and declining precipitation. These climate shifts are expected to result in reduced crop yields and heightened water scarcity, emphasizing the urgent need for proactive adaptation strategies.

In summary, the spatial distribution of climate projections shows regional variations across the basin. The eastern region is projected to experience the highest increases in maximum temperatures, while the western region is anticipated to suffer the most significant declines in precipitation. These findings highlight the critical vulnerability of Jordan’s western agricultural zones and reinforce the need for region-specific climate resilience planning.

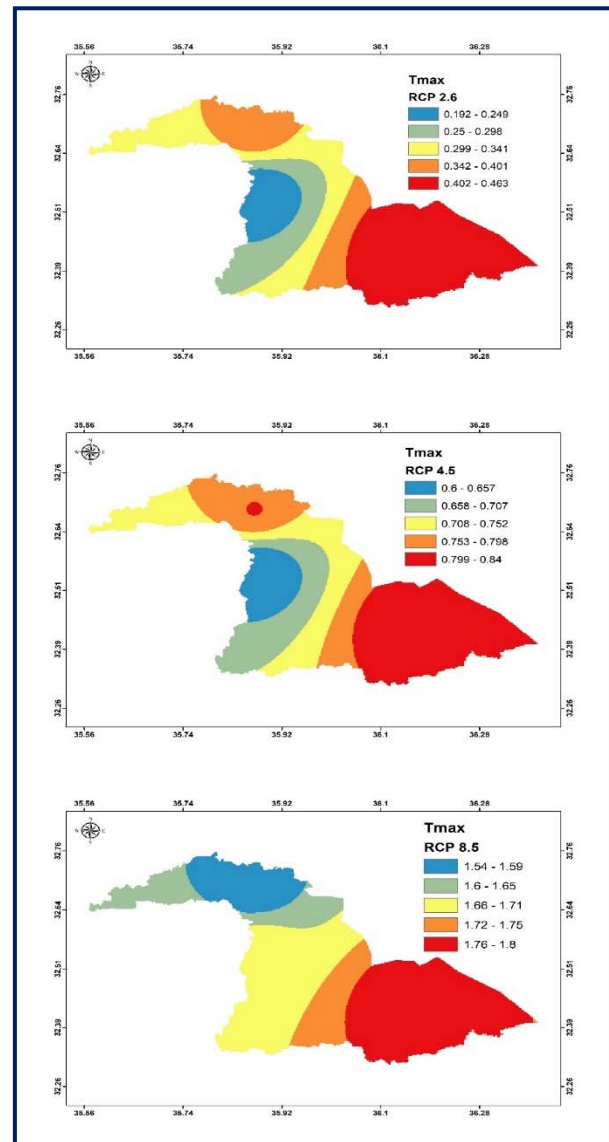


Figure (8): Spatial distribution for the increase in the maximum temperatures during the period 2018-2100

Extreme Climate Change Events Projection

The analysis of future climate scenarios highlights a significant shift in temperature extremes across the basin, emphasizing the intensification of heat events and the decline in cold spells. These changes underscore the profound impact of global warming on regional climate patterns. Table 4 summarizes the projected changes in extreme climate events—heatwaves, cold spells, and consecutive dry days—at Irbid, Al-Mafraq, and Samar stations under the RCP2.6, RCP4.5, and RCP8.5 scenarios.

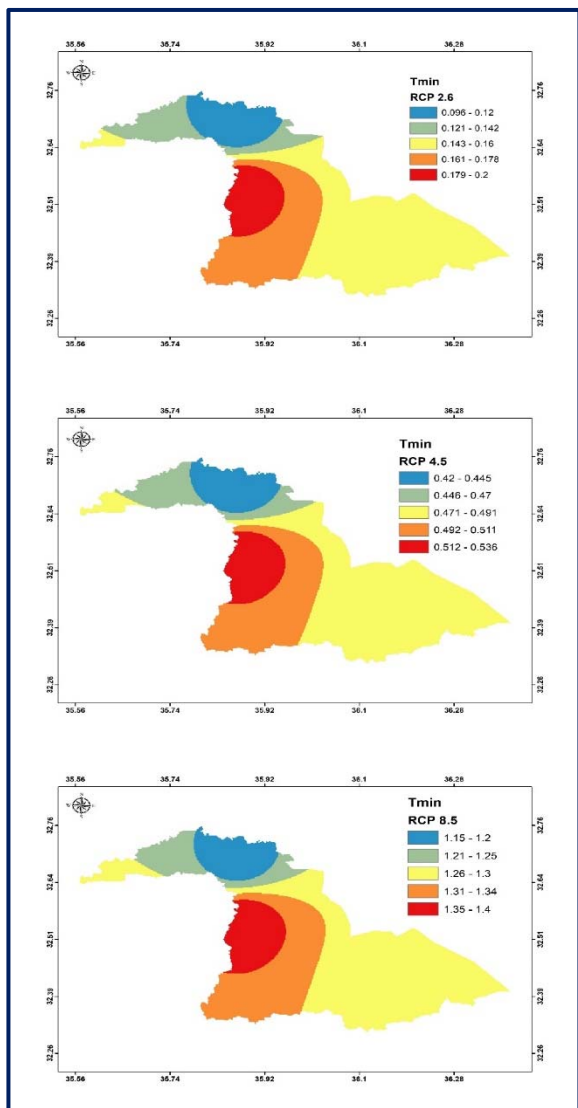


Figure (9): Spatial distribution for the percentage change in the minimum temperature during the period 2018-2100

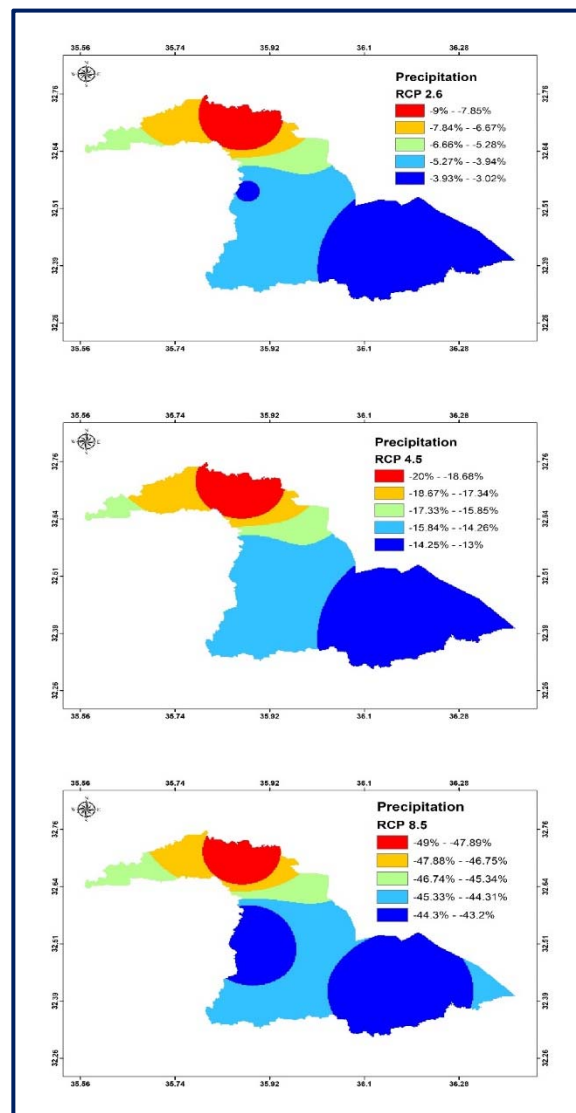


Figure (10): Spatial distribution for the percentage change in precipitation during the period 2018-2100

Heatwaves

Heatwaves are projected to increase significantly across all scenarios, with higher emissions correlating with greater increases. For instance, under RCP2.6, the number of heatwave days is expected to rise by 2.2 days in Irbid and by 2.7 days in both Al-Mafraq and Samar. This trend intensifies under RCP4.5, with increases reaching 8.7 days in Irbid, 7.1 in Al-Mafraq, and 6.6 days in Samar. Under the high-emission RCP8.5 scenarios, the projections show a dramatic rise—up to 22 days in Irbid, 21.9 days in Al-Mafraq, and 17.6 days in Samar. This escalation in extreme heat events presents considerable risks to public health, energy demand, and agricultural productivity.

Cold Spells

In contrast, cold spells are expected to decline substantially. Under RCP2.6, cold spell days are projected to decrease by 3.5 days in Irbid, 2.6 days in Al-Mafraq, and nearly one day in Samar. The decline becomes more pronounced under RCP4.5, with reductions of 11.8 days in Irbid, 9.1 days in Al-Mafraq, and 7.6 in Samar. Under RCP8.5, cold spells diminish even further—by 24.27 days in Irbid, 17.47 days in Al-Mafraq, and 14.78 days in Samar. While milder winters might appear beneficial, the disruption to ecological and agricultural systems, such as pest regulation and crop dormancy, may result in negative cascading effects on bio-diversity and food production.

Consecutive Dry Days

Projected increases in Consecutive Dry Days (CDDs) indicate worsening drought conditions across the basin. Under RCP2.6, Irbid may experience additional 24.1 dry days, while Samar and Al-Mafraq could see increases of approximately 10.5 days and 2.5 days, respectively. Under RCP4.5, the figures rise to 25.7 days in Irbid, 22.3 days in Samar, and 2.8 days in Al-Mafraq. The most severe scenario, RCP8.5, projects 62 additional dry days in Irbid, staggering 65.9 days in Samar, and 3.4 in Al-Mafraq. These patterns highlight the growing aridity and potential decline in soil

moisture, with serious implications for water availability and food security, particularly in already water-scarce regions like Jordan.

In summary, the projected rise in heatwaves, the substantial reduction in cold spells, and the increase in consecutive dry days collectively illustrate the intensifying climate extremes anticipated under future scenarios. These findings emphasize the need for urgent climate adaptation measures tailored to local vulnerabilities in water management, public health, and agricultural resilience.

Table 4. Projected changes in extreme climate events under the RCP scenarios

Parameter	RCP	Irbid (days)	Al-Mafraq (days)	Samar (days)
Heatwaves	RCP2.6	+2.2	+2.7	+2.7
	RCP4.5	+8.7	+7.1	+6.6
	RCP8.5	+22.0	+21.9	+17.6
Cold Spells	RCP2.6	-3.5	-2.6	-0.98
	RCP4.5	-11.8	-9.1	-7.6
	RCP8.5	-24.27	-17.47	-14.78
Consecutive Dry Days	RCP2.6	+24.108	+2.46	+10.496
	RCP4.5	+25.748	+2.8	+22.304
	RCP8.5	+62.074	+3.362	+65.896

Assessment of Climate Conditions for the Period 2006-2017

The CANESM2 GCMs began forecasting and scenario creation in 2006, providing a 12-year period for comparison between the simulated scenarios and observed climatic data. This period allows for an assessment of the basin’s conditions under different scenarios. Figure (11) presents a comparison of the observed maximum temperatures against the downscaled RCP8.5 scenarios for the Irbid station as an example.

The results indicate concerning trends in the Yarmouk River Basin (YRB). Both the observed maximum and minimum temperatures at all stations showed a steeper increase and higher averages compared to the RCP8.5 scenario. Additionally, the observed precipitation exhibited a more significant decline at Samar and Al-Mafraq stations than predicted by the RCP8.5 scenario. These findings suggest a higher likelihood of the basin experiencing a dry phase, with the probability of drought conditions increasing substantially.

Drought Analysis Based on SPI

This part presents a detailed analysis of drought conditions for Irbid, Al-Mafraq, and Samar in YRB using the Standardized Precipitation Index (SPI-12) under three climate change scenarios: RCP2.6 (low emissions), RCP4.5 (moderate emissions), and RCP8.5 (high emissions). The aim is to assess how projected changes in precipitation patterns may influence drought risk and hydro-climatic variability in northern Jordan throughout the 21st century.

The Standardized Precipitation Index (SPI-12) frequency analysis for Irbid under the RCP2.6 scenario (Figure (12)) demonstrates a balanced and stable distribution of wet and dry conditions throughout the 21st century. Approximately 50.85% of the months fall under near-normal to wet conditions ($SPI \geq 0$), while 49.15% correspond to dry conditions ($SPI < 0$), indicating a nearly symmetrical pattern. Extreme drought events ($SPI \leq -2$) make up about 3.08%, a slightly higher percentage than in RCP4.5, but still lower than in RCP8.5, suggesting a limited risk of severe prolonged droughts. Conversely, extremely wet months

($SPI \geq 2$) are rare, appearing in less than 2% of the record. Most SPI values are clustered between -1.5 and +1.5, highlighting the dominance of moderate to near-normal precipitation conditions under this low-emissions pathway. This pattern underscores the

potential benefits of climate mitigation, as RCP2.6 results in fewer extreme events and greater climatic stability for Irbid compared to higher emission scenarios.

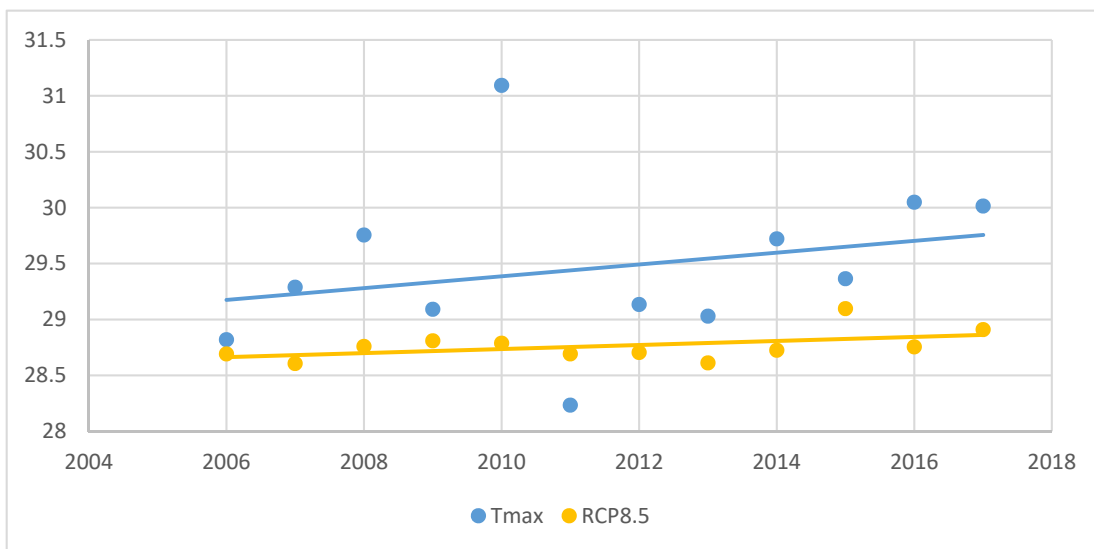


Figure (11): Comparison of observed maximum temperatures against RCP8.5 scenario in Irbid station

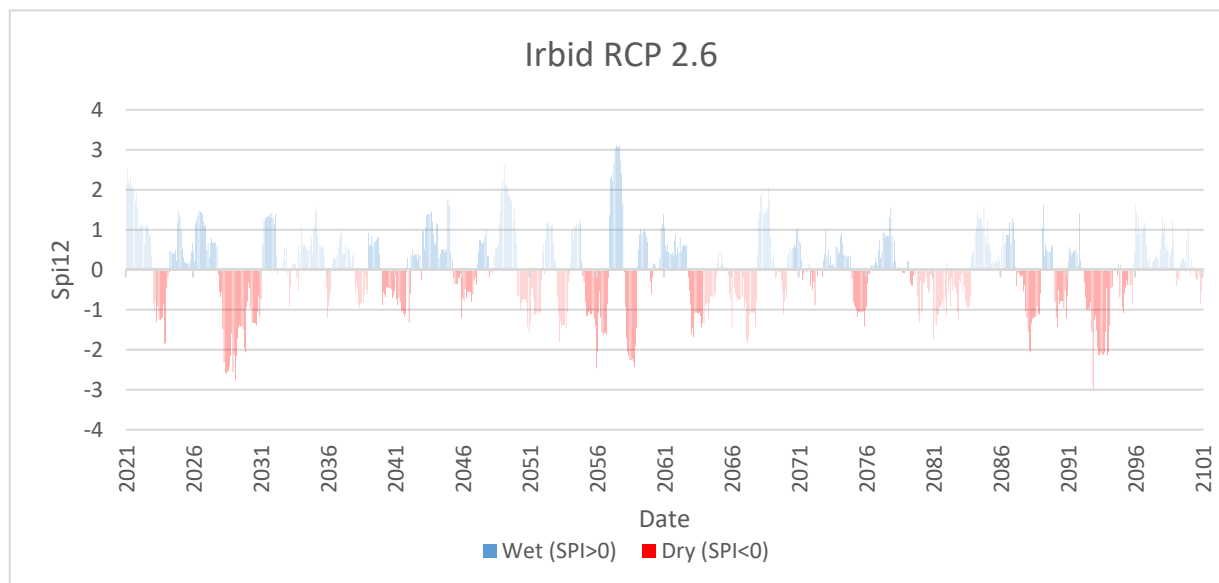


Figure (12): Area chart of standardized precipitation index (SPI-12) from 2020 to 2100 in Irbid under RCP2.6 scenario

Under the RCP4.5 scenario, the SPI-12 frequency distribution (Figure 13)) also shows a generally symmetrical pattern, with dry months ($SPI < 0$) comprising approximately 50.82% of the total. While slightly more inclined toward drought than RCP2.6, this scenario presents a moderate shift. Most SPI values remain within the -1.5 to +1.5 range, suggesting

predominantly near-normal conditions. Extreme drought events ($SPI \leq -2$) are less common, at about 0.72% of months, while extreme wet conditions ($SPI \geq 2.5$) occur slightly more frequently than in RCP8.5, reaching up to $SPI = 3.4$. This scenario reflects a modest increase in hydro-climatic variability compared to RCP2.6, yet it remains considerably less volatile than RCP8.5.

In contrast, the RCP8.5 scenario indicates a more pronounced trend toward dryness in Irbid (Figure (14)). Approximately 40.65% of the months fall below an SPI of -0.5, suggesting persistent dry conditions. Extreme drought events ($SPI \leq -2$) account for about 0.93% of the months, slightly higher than in RCP4.5. While some wet conditions ($SPI \geq 1$) are observed, they are less frequent

and generally less intense than the dry extremes. The dominance of slightly negative SPI values (e.g. -0.5 to 0) highlights the risk of recurrent moderate droughts. Overall, the RCP8.5 scenario projects the driest and most drought-prone future for Irbid, with significant implications for water resources and agricultural stability.

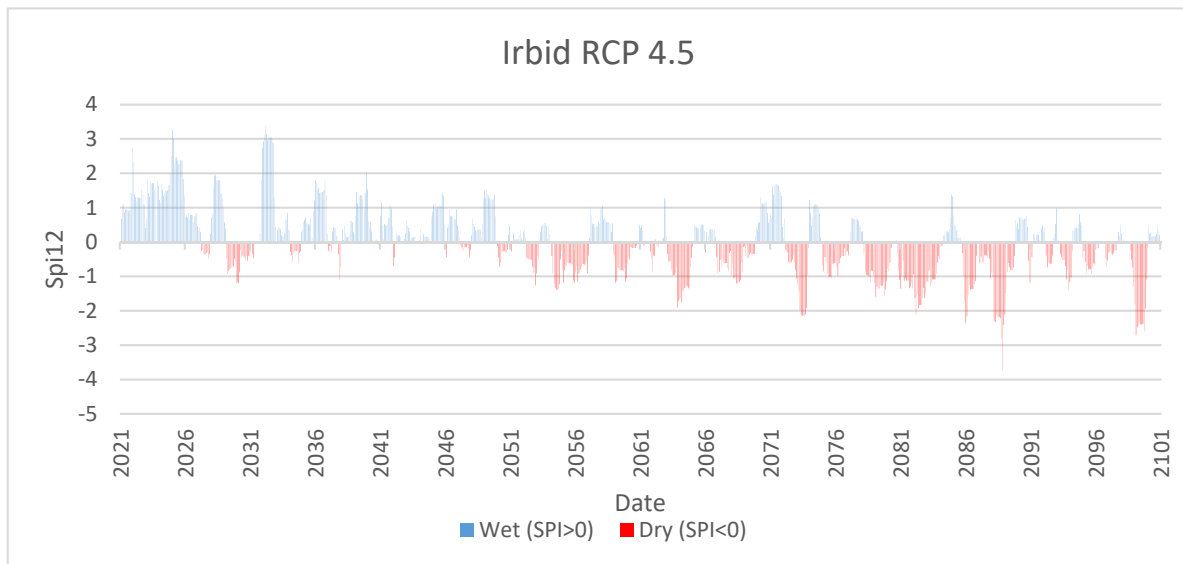


Figure (13): Area chart of standardized precipitation index (SPI-12) from 2020 to 2100 in Irbid under RCP4.5 scenario

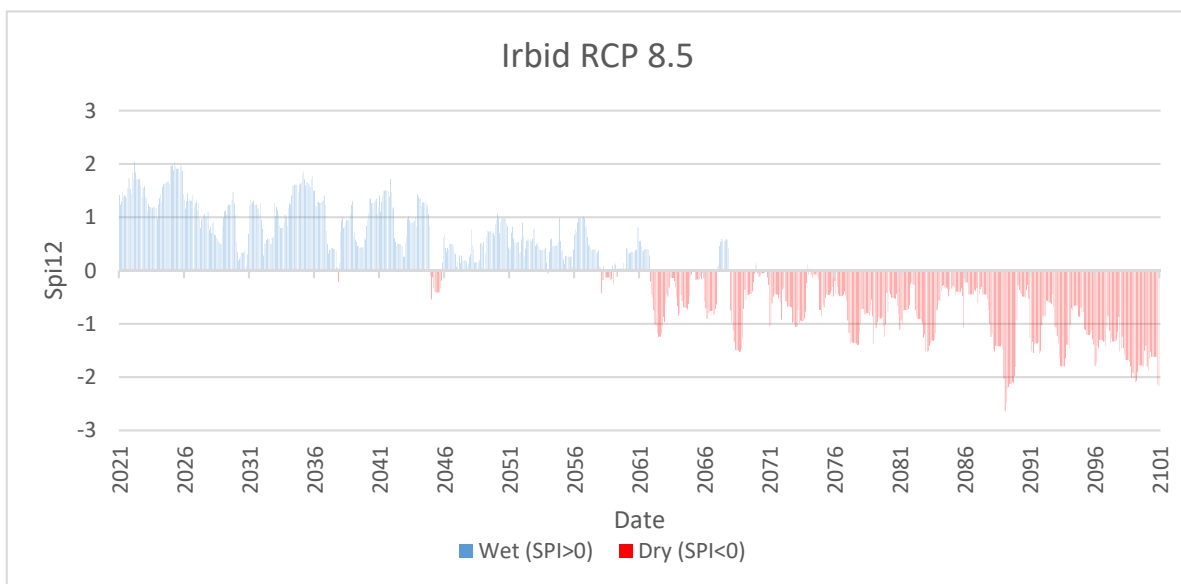


Figure (14): Area chart of standardized precipitation index (SPI-12) from 2020 to 2100 in Irbid under RCP8.5 scenario

The Standardized Precipitation Index (SPI-12) frequency analysis for Al-Mafraq under the RCP 2.6 scenario (Figure (15)) reveals a predominance of dry

conditions throughout the period. Approximately 57.5% of the months are categorized under dry to moderately dry conditions ($SPI < 0$), while about 42.5% fall under

near-normal to wet conditions ($SPI \geq 0$). This distribution indicates a relatively unbalanced climate pattern with a tendency toward drier periods.

Extreme drought events ($SPI \leq -2$) make up about 1.93% of the record, suggesting that severe droughts occur, but are relatively infrequent under the RCP 2.6 scenario. Conversely, extremely wet months ($SPI \geq 2$) are quite rare, constituting just 0.62% of the dataset, which further underscores the scarcity of significantly wet periods in the region. The majority of SPI values are concentrated between -1.5 and +1.5, pointing to a prevalence of moderate to near-normal precipitation levels.

This distribution suggests that Al-Mafraq, under the RCP 2.6 scenario, is likely to experience frequent dry conditions with occasional moderate wet spells. Although extreme wet or dry events remain limited, the region's vulnerability to extended dry periods highlights the importance of water management and drought preparedness. The results also reflect the benefits of the RCP 2.6 scenario, which, despite the higher occurrence of dry conditions, still offers a more balanced climate future compared to higher emission scenarios, like RCP 4.5 or RCP 8.5, where extreme events would likely be more frequent and intense.

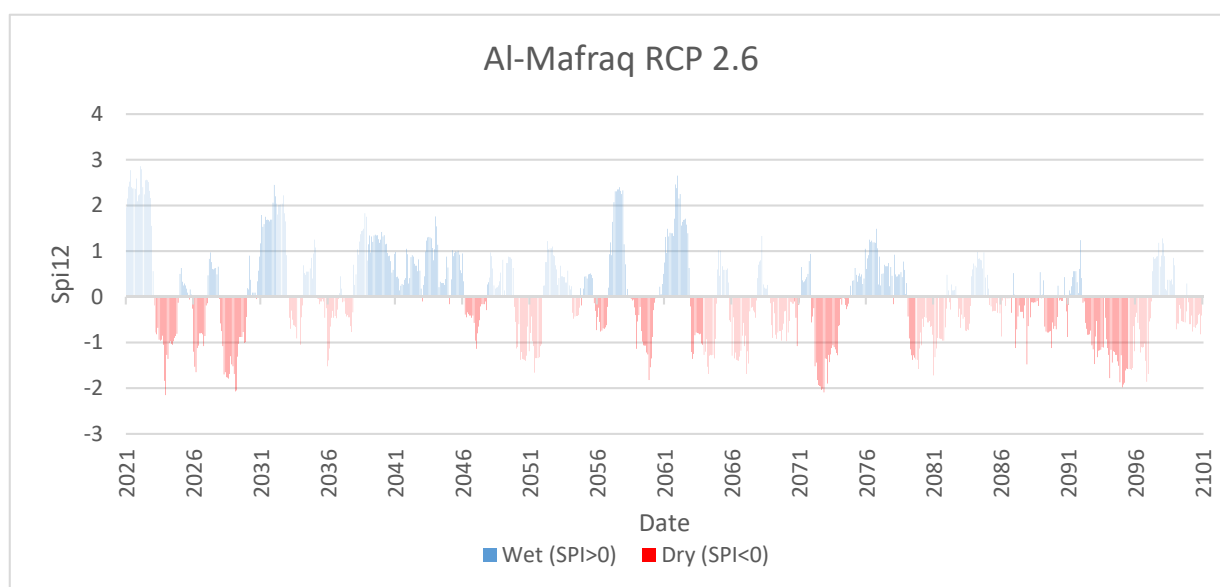


Figure (15): Area chart of standardized precipitation index (SPI-12) from 2020 to 2100 in Al-Mafraq under RCP2.6 scenario

Comparing the RCP 2.6 scenario with RCP 4.5, the SPI-12 frequency analysis for Al-Mafraq under the RCP 4.5 scenario (Figure (16)) reveals a more variable distribution of precipitation. Approximately 54.5% of the months are classified as dry to moderately dry ($SPI < 0$), while 45.5% fall under near-normal to wet conditions ($SPI \geq 0$), showing a relatively balanced, but slightly drier pattern. The increased frequency of both dry and wet conditions highlights the growing variability in the climate under a moderate emission pathway.

Extreme drought events ($SPI \leq -2$) account for about 0.92% of the record, which is slightly higher than under RCP 2.6, but is still pointing to that severe droughts remain rare. On the other hand, extremely wet conditions ($SPI \geq 2$) appear in about 1.51% of the record,

similar to the RCP 2.6 scenario, and are relatively infrequent.

The majority of SPI values are concentrated between -1.5 and +1.5, similar to the RCP 2.6 scenario, but the increased frequency of negative SPI values in this scenario indicates a slightly higher incidence of drier conditions, which may result in a greater risk of drought over time. This suggests a moderate shift toward drier conditions compared to RCP 2.6, with more variability in precipitation levels.

Looking at the highest emission scenario, RCP 8.5 (Figure (17)), the SPI-12 frequency analysis for Al-Mafraq shows a significant shift toward drier conditions compared to the lower emission scenarios (RCP 2.6 and RCP 4.5). Approximately 59.5% of the months are classified as dry to moderately dry ($SPI < 0$), with a

notable frequency of values falling below -1, indicating a clear trend toward drier periods. Conversely, about 40.5% of the months exhibit near-normal to wet

conditions ($SPI \geq 0$), which is lower than the other scenarios, suggesting a reduced frequency of wet conditions.

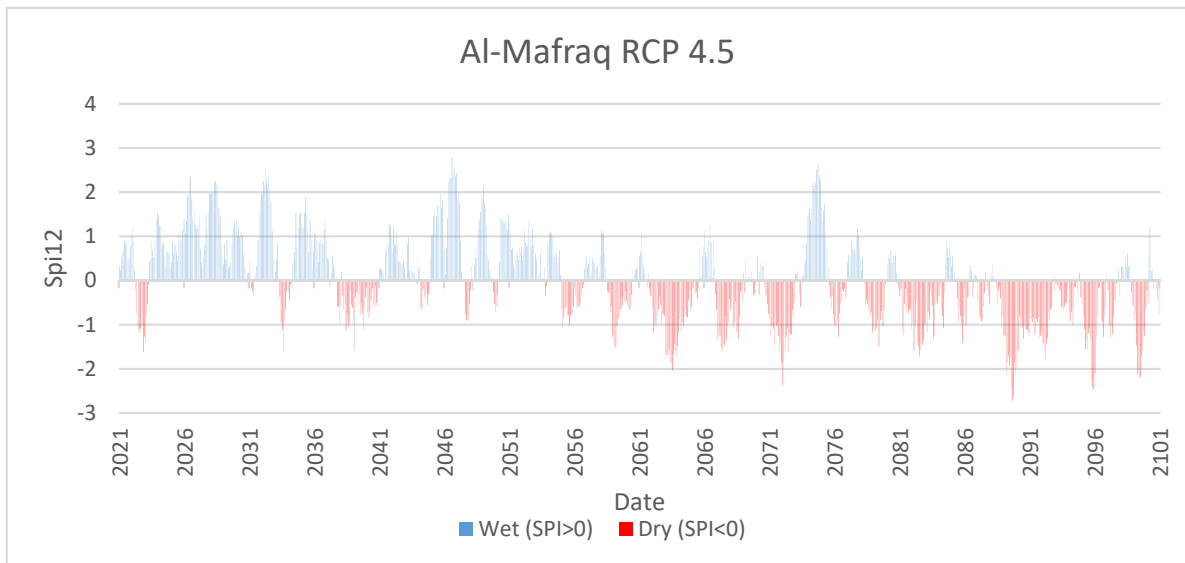


Figure (16): Area chart of standardized precipitation index (SPI-12) from 2020 to 2100 in Al-Mafraq under RCP4.5 scenario

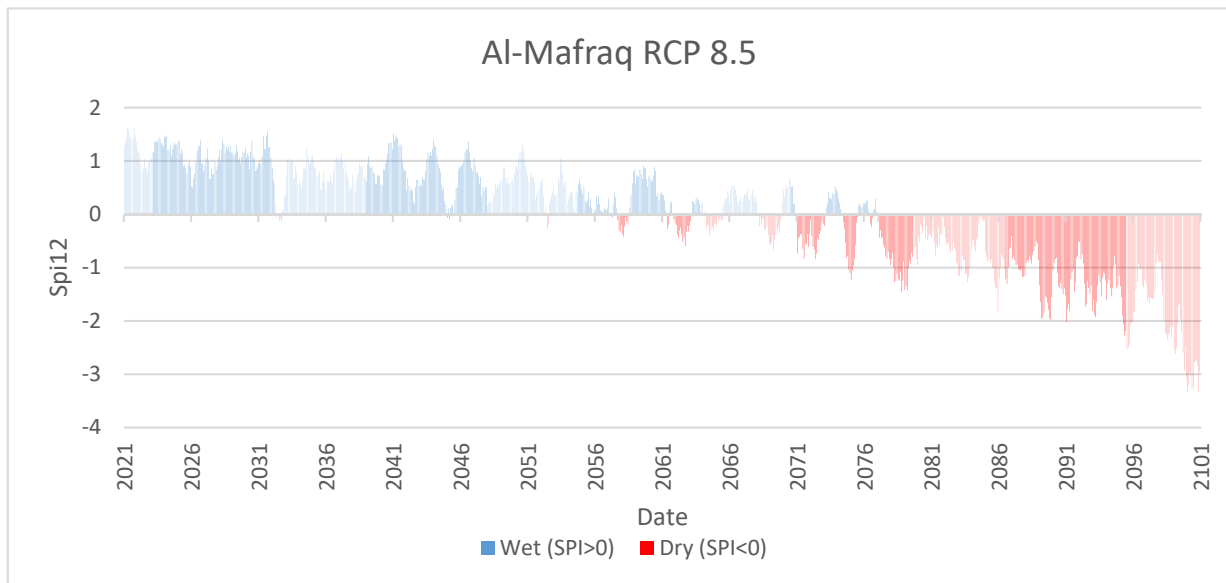


Figure (17): Area chart of standardized precipitation index (SPI-12) from 2020 to 2100 in Al-Mafraq under RCP8.5 scenario

Extreme drought events ($SPI \leq -2$) make up approximately 3.92% of the record, a value notably higher than the RCP 2.6 and RCP 4.5 scenarios, reflecting an increased risk of prolonged droughts in this high-emissions pathway. Extreme wet conditions ($SPI \geq 2$) are relatively infrequent, appearing in just 0.82% of the months, which is consistent with the lower frequency

of wet events observed in other scenarios.

The majority of SPI values fall between -1.5 and +1.5, indicating that most months are characterized by moderate precipitation conditions. However, the higher frequency of negative SPI values in the RCP 8.5 scenario compared to the RCP 2.6 and RCP 4.5 scenarios highlights a trend of more frequent dry spells,

with more severe drought events becoming a real possibility as emissions increase.

The Standardized Precipitation Index (SPI-12) frequency analysis for Samar under the RCP 2.6 scenario (Figure (18)) reveals a distribution of precipitation conditions that shows a tendency toward dry conditions, with a significant frequency of both dry and near-normal months.

Approximately 53.4% of the months are categorized under dry to moderately dry conditions ($SPI < 0$), while 46.6% fall under near-normal to wet conditions ($SPI \geq 0$). This distribution indicates a relatively balanced climate pattern, but with a tendency for drier periods. Extreme drought events ($SPI \leq -2$) account for about 2.1% of the record, suggesting that severe droughts are infrequent under this scenario. Extremely wet conditions ($SPI \geq 2$) are observed in just 2.0% of the months, highlighting that significant wet events remain rare.

The majority of SPI values are concentrated between -1.5 and +1.5, indicating that most months experience moderate precipitation levels. While dry spells are more frequent, the region is still expected to experience periodic wet months. This suggests that under the RCP 2.6 scenario, Samar is likely to face frequent dry conditions with occasional moderate wet spells, although extreme wet or dry events remain limited.

Comparing RCP 2.6 with RCP 4.5 (Figure (19)), the SPI-12 frequency analysis for Samar under the RCP 4.5

scenario reveals a more variable precipitation pattern. Approximately 53.1% of the months fall under dry to moderately dry conditions ($SPI < 0$), while 46.9% are classified as near-normal to wet ($SPI \geq 0$). This shows a relatively balanced, yet slightly drier, climate compared to RCP 2.6, with an increased frequency of both dry and wet conditions, suggesting greater climate variability under a moderate emission pathway.

Extreme drought events ($SPI \leq -2$) make up about 1.5% of the record, slightly lower than under RCP 2.6, which indicates that severe droughts remain rare. Conversely, extremely wet conditions ($SPI \geq 2$) occur in 3.1% of the months, slightly higher than in the RCP 2.6 scenario, although still being relatively infrequent.

The majority of SPI values are concentrated between -1.5 and +1.5, with a slight shift toward drier conditions compared to RCP 2.6. This suggests a moderate shift toward drier conditions, with increased variability in precipitation, highlighting the potential for a greater risk of drought over time.

Under the highest emission scenario, RCP 8.5 (Figure (20)), the SPI-12 frequency analysis for Samar shows a significantly more extreme precipitation pattern compared to RCP 2.6 and RCP 4.5. Approximately 50.5% of the months are categorized as dry to moderately dry ($SPI < 0$), while 49.5% fall under near-normal to wet conditions ($SPI \geq 0$), indicating an even split between drier and wetter months.

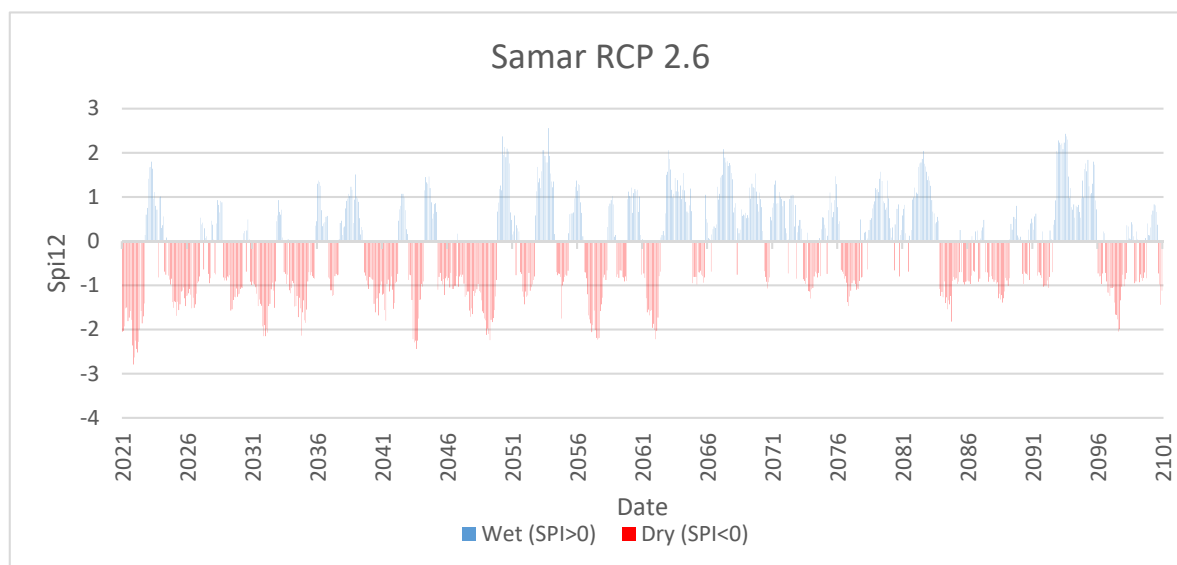


Figure (18): Area chart of standardized precipitation index (SPI-12) from 2020 to 2100 in Samar under RCP2.6 scenario

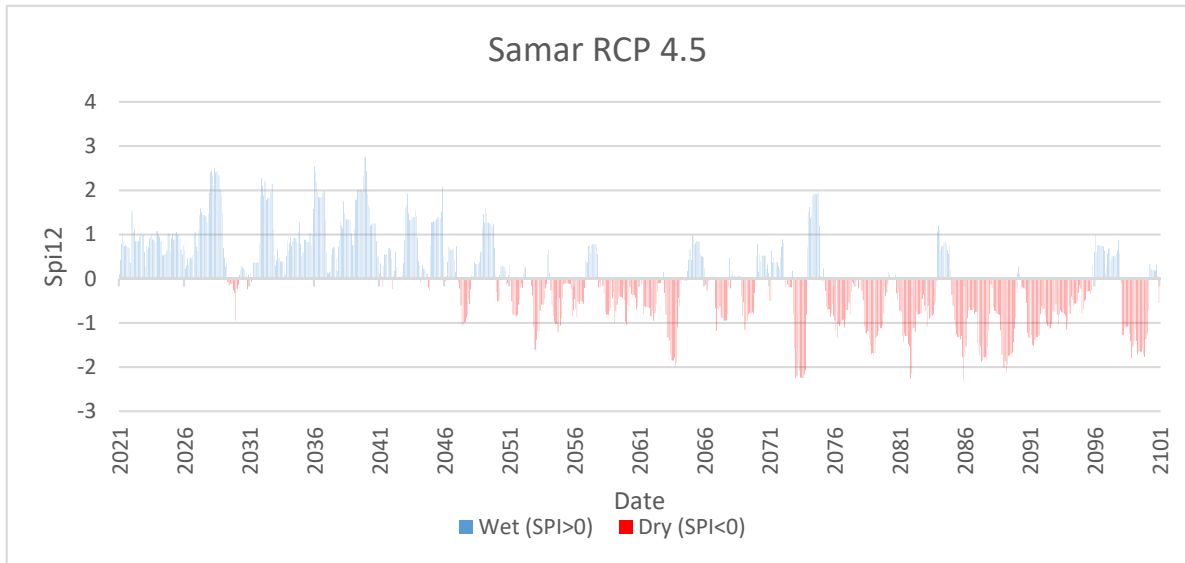


Figure (19): Area chart of standardized precipitation index (SPI-12) from 2020 to 2100 in Samar under RCP4.5 scenario

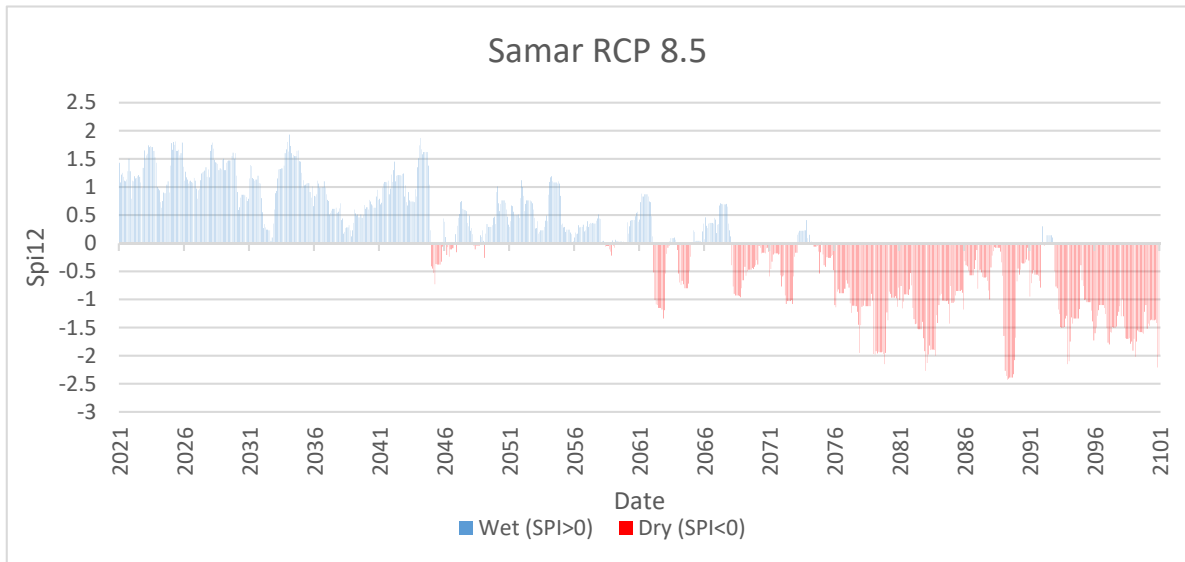


Figure (20): Area chart of standardized precipitation index (SPI-12) from 2020 to 2100 in Samar under RCP8.5 scenario

Extreme drought events ($SPI \leq -2$) account for about 1.56% of the months, showing a noticeable increase compared to the lower emission scenarios, indicating a higher likelihood of extreme dry events. On the other hand, extremely wet conditions ($SPI \geq 2$) appear in 7.8% of the months, significantly higher than in both RCP 2.6 and RCP 4.5, suggesting a higher frequency of extremely wet events.

The majority of SPI values are concentrated between -1.5 and +1.5, indicating that most months experience moderate precipitation levels. However, the higher frequency of both dry and wet extremes under RCP 8.5

emphasizes a more volatile climate, with pronounced periods of both drought and heavy rainfall.

Taken together, the results for Irbid show a clear gradient: RCP2.6 offers the most stable and favorable climate outlook, while RCP4.5 indicates moderate, but manageable, variability. In contrast, RCP8.5 projects a significantly drier and more drought-prone future. These findings highlight the critical importance of aggressive climate mitigation in reducing future hydro-climatic risks for northern Jordan.

For Al-Mafraq, the SPI data across all RCP scenarios shows a clear shift toward drier and more volatile

conditions as emissions increase. Although extremely wet events remain rare, the risk of extreme droughts rises notably in higher emission scenarios, emphasizing the need for adaptive water management strategies to manage increasing precipitation variability and ensure long-term sustainability in the region.

Similarly, the SPI-12 frequency analysis for Samar across the three RCP scenarios reveals a shift toward more extreme precipitation conditions as emissions increase. While dry conditions predominate across all scenarios, the frequency of both extremely wet and dry events rises with higher emissions, particularly under the RCP 8.5 scenario. This further underscores the importance of developing adaptive strategies that can address both the growing risk of severe droughts and the potential for extremely wet events in a higher emission future.

CONCLUSIONS

In this research, CanESM2 was used within the Statistical Downscaling Model (SDSM) to downscale maximum temperature, minimum temperature, and precipitation at three sub-regions (each with one temperature and one precipitation station) on the Jordanian side of the Yarmouk River Basin (YRB). From our analysis, the following conclusions emerge:

1. **High Modeling Accuracy:** SDSM–CanESM2 achieved excellent performance in simulating the arid climate of the YRB (calibration R^2 : 0.87–0.996; validation R^2 : 0.799–0.998), confirming SDSM’s suitability for semi-arid and arid climate modeling.
2. **Persistent Warming and Drying Trends:** Under all RCP scenarios (2.6, 4.5, 8.5), projected maximum and minimum temperatures continue to rise through 2100, while precipitation steadily declines, amplifying water-scarcity pressures.
3. **Spatial Variability of Impacts:** The eastern sub-region faces the greatest increases in maximum temperature, whereas the agriculturally vital western sub-region endures the largest precipitation reductions—intensifying regional disparities in

water availability and crop stress.

4. **Growing Climate Instability:** Future projections show more frequent heatwaves, fewer cold spells, and longer sequences of Consecutive Dry Days (CDDs), signaling elevated risks to public health, ecosystems, and water resources.
5. **Elevated Drought Risk beyond RCP8.5 Expectations:** Observed trends already exceed RCP8.5 projections, indicating that the YRB is experiencing faster warming and sharper precipitation declines than even the high-emission scenario predicts—underscoring an urgent need for mitigation.
6. **Scenario-dependent Drought Frequency:** SPI-12 analysis reveals that under RCP2.6, drought and wet months remain balanced (~50/50%) with low extreme-drought frequencies (1–3%), whereas RCP8.5 drives over 40% of months into dry conditions and up to ~4% extreme-drought frequency, especially at Irbid and Al-Mafraq, with Samar also experiencing spikes in extremely wet events.
7. **Recommendation for Adaptation and Modeling:** Given SDSM’s robust performance, we recommend its continued use for projecting hydro-climatic change in semi-arid and arid regions. Targeted adaptation measures—enhanced water storage, optimized irrigation, and drought-tolerant crops—are critical under all scenarios, but especially under high-emission pathways. Aggressive mitigation (RCP2.6) can substantially reduce future drought risk and ease the scale of adaptation needed.

These findings highlight the combined importance of emission reduction and region-specific adaptation to safeguard water security and agricultural resilience in the Yarmouk River Basin.

Acknowledgements

Grateful thanks are due for the support awarded by the Deanship of Scientific Research at Al-Balqa Applied University for the conduction of this research.

REFERENCES

- Abdulla, F. (2020). "21st century climate change projections of precipitation and temperature in Jordan". *Procedia-Manufacturing*, 44, 197-204.
- Abdulla, F.A., Al-Shurafat, A.W., and Shawaqfah, M.S. (2021). "Statistically downscaling climate change projection of precipitation and temperature over the semi-arid Yarmouk Basin, Jordan". *International Journal of Global Warming*, 24 (3/4), 261-280. <https://doi.org/10.1504/IJGW.2021.116709>
- Al-Bakri, J., Suleiman, A., Abdulla, F., and Ayad J. (2011). "Potential impact of climate change on rainfed agriculture of a semi-arid basin in Jordan". *Physics and Chemistry of the Earth, Parts A/B/C* 36(5-6):125-134. <https://doi.org/10.1016/j.pce.2010.06.001>
- Allen, R.G., Pereira, L.S., Raes, D., and Smith, M. (1998). "Crop evapotranspiration: Guidelines for computing crop water requirements". *FAO Irrigation and Drainage Paper* 56. FAO, Rome, 300(9), D05109.
- Al Qatarnah, G.N., Al Smadi, B., Al-Zboon, K. et al. (2018). "Impact of climate change on water resources in Jordan: A case study of Azraq basin". *Appl. Water Sci.*, 8, (50). <https://doi.org/10.1007/s13201-018-0687-9>
- Al Qatarnah, Ghada, and Kamel K. Al-Zboon, (2022), "Water poverty index: A tool for water resource management in Jordan". *Water Air Soil Pollut.*, (2022) 233:461 <https://doi.org/10.1007/s11270-022-05892-3>
- Alzboon, K.K., La'aly, A., and Alrawashdeh, K.A.B. (2021). "Climate change indicators in Jordan: A new approach using area method". *Jordan Journal of Civil Engineering*, 15 (1).
- Barjenbruch, M., and Alzboon, K.K. (2010). "North-south gap in wastewater management: A comparative study for Germany and Jordan. *Global Warming: Engineering Solutions*, 545-554.
- Bashabsheh, A. Q., and Alzboon, K.K. (2024). "Impact of climate change on water resources in the Yarmouk River Basin of Jordan". *Journal of Arid Land*, 16 (12), 1633-1647. <https://doi.org/10.1007/s40333-024-0069-0>
- Clarke, L., Jiang, K., Akimoto, K., et al. (2014). "Chapter 6: Assessing transformation pathways". In: *Climate Change 2014: Mitigation of Climate Change*". IPCC Working Group III Contribution to AR5. Cambridge University Press.
- Dibike, Y.B., Gachon, P., St-Hilaire, A., Ouarda, T.B., and Nguyen, V.T.V. (2008). "Uncertainty analysis of statistically downscaled temperature and precipitation regimes in northern Canada". *Theoretical and Applied Climatology*, 91, 149-170.
- El Raey, M., and El Hadidi, A. (2016). "Modeling of climatological conditions over the past century in Alexandria, Egypt". *International Journal of Sciences*, 5 (07), 1-10.
- Fan, X., Jiang, L., and Gou, J. (2021). "Statistical downscaling and projection of future temperatures across the Loess Plateau, China". *Weather and Climate Extremes*, 32, 100328.
- FAO, Food and Agriculture originations. (2023). "Geography and population". <https://www.fao.org/4/W4356E/w4356e0f.HTM>
- Fowler, H.J., Blenkinsop, S., and Tebaldi, C. (2007). "Linking climate change modeling to impact studies: Recent advances in downscaling techniques for hydrological modeling". *Climatology*, 27, 1547-1578.
- Giorgi, F., and Lionello, P. (2008). "Climate change projections for the Mediterranean region". *Global and Planetary Change*, 63 (2-3), 90-104. <https://doi.org/10.1016/j.gloplacha.2007.09.005>
- Hargreaves, G.H., and Samani, Z.A. (1985). "Reference crop evapotranspiration from temperature". *Applied Engineering in Agriculture*, 1 (2), 96-99.
- Hashmi, M.Z., Shamseldin, A.Y., and Melville, B.W. (2011). "Comparison of SDSM and LARS-WG for simulation and downscaling of extreme precipitation events in a watershed". *Stochastic Environmental Research and Risk Assessment*, 25 (4), 475-484.
- Hassan, W.H. (2020). "Climate change impact on groundwater recharge of Umm er Radhuma unconfined aquifer western desert, Iraq". *International Journal of Hydrology Science and Technology*, 10 (4), 392-412.
- Huang, J., Zhang, J., Zhang, Z., Xu, C., Wang, B., and Yao, J. (2011). "Estimation of future precipitation change in the Yangtze River basin by using the statistical downscaling method". *Stochastic Environmental Research and Risk Assessment*, 25 (6), 781-792.
- IPCC. (2021). "Climate change 2021". Working Group I Contribution to the Sixth Assessment Report of the Intergovernmental Panel on Climate Change. https://report.ipcc.ch/ar6/wg1/IPCC_AR6_WGI_FullReport.pdf

- IPCC. (2022). "Annex I: Glossary". In: Global Warming of 1.5°C: IPCC Special Report on Impacts of Global Warming of 1.5°C above Pre-industrial Levels in the Context of Strengthening Response to Climate Change, Sustainable Development, and Efforts to Eradicate Poverty (pp. 541-562). Cambridge: Cambridge University Press. [Doi:10.1017/9781009157940.008](https://doi.org/10.1017/9781009157940.008)
- Kottek, M., Grieser, J., Beck, C., Rudolf, B., and Rubel, F. (2006). "World map of the Köppen-Geiger climate classification updated". *Meteorologische Zeitschrift*, 15 (3), 259-263. <https://doi.org/10.1127/0941-2948/2006/0130>
- Kumar, S., Kinter, J., Dirmeyer, P.A., Pan, Z., and Adams, J. (2013). "Multi-decadal climate variability and the "warming hole" in north America: Results from CMIP5 twentieth- and twenty-first-century climate simulations". *Journal of Climate*, 26 (11), 3511-3527. <https://doi.org/10.1175/JCLI-D-12-00535.1>
- Langsdorf, S., Lösckke, S., Möller, V., Okem, A., Officer, S., Rama, B., Belling, D., Dieck, W., Götze, S., Kersher, T., Mangele, P., Maus, B., Mühle, A., Nabyeva, K., Nicolai, M., Niebuhr, A., Petzold, J., Prentzler, E., Savolainen, J., and Scheuffele, H. (2022). "Climate change 2022: Impacts, adaptation and vulnerability". Working Group II Contribution to the Sixth Assessment Report of the Intergovernmental Panel on Climate Change. IPCC. <https://doi.org/10.1017/9781009325844>
- Leduc, M., Mailhot, A., Frigon, A., Martel, J.L., Ludwig, R., Brietzke, G. B., ..., and Scinocca, J. (2019). "The ClimEx project: A 50-member ensemble of climate change projections at 12-km resolution over Europe and northeastern North America with the Canadian Regional Climate Model (CRCM5)". *Journal of Applied Meteorology and Climatology*, 58 (4), 663-693.
- Linares, C., Díaz, J., Negev, M., Martínez, G.S., Debono, R., and Paz, S. (2020). "Impacts of climate change on the public health of the Mediterranean Basin population: Current situation, projections, preparedness and adaptation". *Environmental Research*, 182, 109107. <https://doi.org/10.1016/j.envres.2019.109107>
- National Drought Mitigation Center (NDMC). (2018). "SPI Generator" [software]. University of Nebraska-Lincoln. <https://drought.unl.edu/Monitoring/SPI/SPIProgram.aspx>
- Raggad, M., Salameh, E., Magri, F., Siebert, C., Roediger, T., and Moller, P. (2016). "Groundwater recharge in a semi-arid environment under high climatic variability and overpumping: Ajlun Highlands as an example, Jordan". In: EGU General Assembly Conference Abstracts. p. 10292.
- Rana, M.M., and Adhikary, S.K. (2024). "Impact of climate change on precipitation and temperature changes in the northwest region of Bangladesh using SDSM: A comparison of CanESM2 and HadCM3 models". *Journal of Engineering Science*, 14 (2), 127-136. <https://doi.org/10.3329/jes.v14i2.71236>
- Saha, S., Moorthi, S., Pan, H. L., Wu, X., Wang, J., Nadiga, S., ..., and Goldberg, M. (2010). "The NCEP climate forecast system re-analysis". *Bulletin of the American Meteorological Society*, 91 (8), 1015-1058.
- Stiliyanova, Anastasiya, Gianni Bellocchi, David Borrás, Ulrich Eza, Raphaël Martin, and Pascal Carrère. (2017). "Kriging-based approach to predict missing air temperature data". *Computers and Electronics in Agriculture*, Volume 142, Part A, 2017, 142, 440-449, The National Climate Change Adaptation Plan of Jordan. (2021). http://www.moenv.gov.jo/ebv4.0/root_storage/ar/eb_list_page/final_draft_nap-2021.pdf
- Tryhorn, L., and DeGaetano, A. (2013). "A methodology for statistically downscaling seasonal snow cover characteristics over the northeastern United States". *International Journal of Climatology*, 33 (12), 2728-2743.
- United Nations. (2022). "What is climate change?" <https://www.un.org/en/climatechange/what-is-climate-change>
- United States Agency for International Development (USAID). (2017). "Climate change risk profile: Jordan factsheet". https://www.climatelinks.org/sites/default/files/asset/document/2017_USAID_Climate%20Change%20Risk%20Profile_Jordan.pdf
- Wilby, R.L., and Dawson, C.W. (2004). "Using SDSM, version 3.1: A decision support tool for the assessment of regional climate change impacts—User manual". Environment Agency of England and Wales and Loughborough University.
- Wilby, R.L., Charles, S.P., Zorita, E., Timbal, B., Whetton, P., and Mearns, L.O. (2004). "Guidelines for use of climate scenarios developed from statistical downscaling methods". Supporting Material of the Intergovernmental Panel on Climate Change. DDC of IPCC TGCIA, 27.

Wilby, R.L., Dawson, C.W., and Barrow, E.M. (2002). "SDSM: A decision support tool for the assessment of regional climate change impacts". *Environmental Modeling and Software*, 17 (2), 145-157.

Wilby, R.L., Dawson, C.W., and Barrow, E.M. (2007). "SDSM 4.2: A decision support tool for the assessment of regional climate change impacts (user manual)". Climate Impacts and Adaptation Research Program.

World Meteorological Organization (WMO). (2012). "Standardized precipitation index user guide (WMO-No. 1090). Geneva, Switzerland". World Meteorological Organization.

World Meteorological Organization (WMO). (2022). "United in science 2022". https://library.wmo.int/doc_num.php?explnum_id=11308